

Self-oscillation Based Identification and Heading Control for Unmanned Surface Vehicles

Marco Bibuli^a, Gabriele Bruzzone^a, Massimo Caccia^a, Nikola Miskovic^b
and Zoran Vukic^b

^a*Consiglio Nazionale delle Ricerche, ISSIA, Via de Marini 6, Genova, Italy*
E-mail: {marco, gabry, max}@ge.issia.cnr.it

^b*Faculty of Electrical Engineering and Computing, University of Zagreb, Unska 3,
Zagreb, Croatia*
E-mail: {nikola.miskovic, zoran.vukic}@fer.hr

Abstract. The paper demonstrates the use of self-oscillation identification method for heading controller tuning of the autonomous unmanned surface vehicle (USV) Charlie. In short, the theory behind self-oscillation identification method is addressed and a model based controller design is described. Two controllers are implemented on the vehicle: controller with Euler backward differentiator for yaw rate calculation, Kalman filter based yaw rate estimator. The Kalman filter is also tuned on the basis of the identified model. The methodology for auto-tuning experiment has been described and implemented on the actual vehicle. The experimental results prove that the proposed method is easily implemented, non time-consuming and gives satisfactory results.

Keywords. Identification, Motion Control

1. Introduction

Determining a model of marine vehicles is a very time-consuming process. However, in order to have autonomy, basic control which includes heading, depth (for underwater vehicles) and surge control, has to be implemented. Procedures for identification of underwater vehicles models are reported in Ridaoui et al. (2004), Caccia et al. (2000), Stipanov et al. (2007), Miskovic et al. (2007a), while some results on autonomous surface marine vehicles in Caccia et al. (2006). All these procedures are based on running numerous steady-state experiments in order to determine the vehicle's drag. In addition to that, vehicle's inertia can be determined by using zig-zag manoeuvres, Caccia et al. (2006), or open-loop transient characteristics, Stipanov et al. (2007).

Having this in mind, in Miskovic et al. (2007c) a much faster identification method has been proposed and implemented on underwater vehicles. The proposed experiment gives responses similar to those of a zig-zag experiment - the difference is in using the describing function theory to determine nonlinear model parameters. This paper uses the same self-oscillations identification method, which will be described later, and de-

scribes the implementation on Charlie USV together with the controller design based on the identified model. Using the proposed procedure, experiments are performed automatically and with desired precision.

Section I gives a short introduction, presents the basic characteristics and mathematical model of Charlie USV and describes the self-oscillation identification method used on the proposed system. Section II gives design procedure of the heading controller design and a short stability analysis. The proposed controller compensates for the nonlinearities in the system and its parameters are determined based on the model transfer function and the parameters identified using the proposed self-oscillation identification method. Section III describes the implementation issues: different controller types and automated self-oscillation monitoring and execution system. Experimental results are presented in Section IV and the paper is concluded with Section V.

1.1. Charlie USV

The Charlie USV (see Fig. 1) is a small catamaran-like shape prototype vehicle originally developed by the CNR-ISSIA for the sampling of the sea surface microlayer and immediate subsurface for the study of the sea-



Fig. 1. Unmanned surface vehicle Charlie.

air interaction Caccia et al. (2005). Charlie is 2.40 m long, 1.70 m wide and weighs about 300 kg in air. The vehicle is equipped with a rudder-based steering system, where two rigidly connected rudders, positioned behind the thrusters, are actuated by a brushless DC motor. The navigation instrumentation set is constituted of a GPS Ashtech GG24C integrated with compass KVH Azimuth Gyrotrac able to compute the True North. The on-board real-time control system, developed in C++, is based on GNU/Linux and run on a Single Board Computer (SBC), which supports serial and Ethernet communications and PC-104 modules for digital and analog I/O.

For dynamic description, a *practical* model for the vehicle has been defined in Caccia et al. (2006). The identified model is consistent, from the point of view of degree of accuracy, quality in terms of noise and sampling rate of the measurements. The experiments have shown that the sway speed can be neglected, thus we give here the yaw model of the vehicle with (1)

$$I_r \dot{r} = \tilde{k}_{r|r} r |r| + n^2 \delta \quad (1)$$

where n is the propeller revolution rate, δ is the rudder angle, \tilde{I}_r is moment of inertia, $\tilde{k}_{r|r}$ is linear drag coefficient. Since in equation (1), the steering torque $n^2 \delta$ has been identified as function of the propeller revolution rate instead of the advance speed, the rudder action is neglected when the vehicle is still moving while n is zero. Thus, the field of validity of the proposed model of vehicle dynamics is for $n > \tilde{n} > 0$. More information on the modeling of the Charlie vehicle could be found in Caccia et al. (2006). The yaw torque control is performed by controlling the rudder angle δ while propeller revolution rate n is kept constant.

1.2. Identification by Use of Self-Oscillations

The idea of using self-oscillations to determine system parameters is described in detail in Miskovic et al. (2007b),

while its application to autonomous underwater vehicles has been described in Miskovic et al. (2007c). A thorough heading and depth controller design based on the self-oscillation identification method has been described in Miskovic et al. (2008) using simulation models of FALCON and VideoRay Automarine AUVs. The self-oscillation experiment is done in closed-loop which consists of the process itself and a nonlinear element. The method is based upon forcing the system into self-oscillations - the magnitude and frequency of the obtained self-oscillations can be used to determine the process' parameters. The link between the space of process' parameters and the space of magnitudes and frequencies of self-oscillations is the Goldfarb principle (see Vukic et al. (2003)). The self-oscillations identification method can be used to determine parameters of linear and nonlinear models under the assumption that the model structure is known. The nonlinear element which is usually used is relay with hysteresis.

Using the proposed method, parameters \tilde{I}_r and \tilde{k}_{rr} in a system described with (1) can be determined using (2) and (3) (see Miskovic et al. (2007c)).

$$\tilde{I}_r = \frac{P_N(X_m)}{\omega^2} \quad (2)$$

$$\tilde{k}_{rr} = -\frac{3\pi Q_N(X_m)}{8 X_m \omega^2} \quad (3)$$

In (2) and (3) ω is the frequency and X_m magnitude of self-oscillations, $P_N(X_m)$ and $Q_N(X_m)$ are real and imaginary parts of the describing function of the nonlinear element respectively. For the relay with hysteresis

$P(X_m) = \frac{4C}{\pi X_m} \sqrt{1 - \left(\frac{x_a}{X_m}\right)^2}$ and $Q(X_m) = -\frac{4C}{\pi X_m^2} x_a$, where C is relay output, and x_a relay width, Vukic et al. (2003). In the case of Charlie USV relay output is yaw torque $n^2 \delta$.

The main assumptions that are posed on given equations are that the oscillations are symmetric and that higher harmonics are negligible in comparison to the first harmonic. Due to asymmetry in the Charlie USV or a constant disturbance, a constant term τ^* can appear in (1) causing the induced self-oscillations to be asymmetric. The constant term τ^* can be determined using equation (4) where T_H and T_L are the times relay output is high and low during one oscillation, respectively. If the constant term exists, it can be compensated within the controller. For details the reader is referred to Miskovic et al. (2008).

$$\tau^* = \delta n^2 \frac{T_H - T_L}{T_H + T_L} \quad (4)$$

When the self-oscillation experiment is conducted on a discrete time system some modifications must be made, see Miskovic et al. (2007b).

2. Controller design

The controller that is used in this paper is a I-PD controller given with equation (5), Vukic and Kuljaca (2005). This controller is appropriate for control due to smooth controller output.

$$\tau_N(t) = K_I \int_0^t [\Psi_{ref}(t) - \Psi(t)] dt - K_P \Psi(t) - K_D \dot{\Psi}(t) \quad (5)$$

In order to compensate the nonlinearity, the steering equation can be written in form (6) where $\varepsilon = k_{rr} |\dot{\Psi}|$.

$$I_r \ddot{\Psi}(t) + \varepsilon \dot{\Psi}(t) = \tau_N(t), \quad (6)$$

Using the proposed control algorithm, the closed loop equation is

$$\frac{\Psi}{\Psi_{ref}} = \frac{1}{\frac{\alpha}{K_I} s^3 + \frac{\varepsilon + K_D}{K_I} s^2 + \frac{K_P}{K_I} s + 1}. \quad (7)$$

The controller parameters are set so that the closed-loop transfer function is equal to the model function $G_m(s) = \frac{1}{a_3 s^3 + a_2 s^2 + a_1 s + 1}$ which is stable. In that case, the controller parameters are given with (8), (9) and (10) where tilde denotes the parameters obtained using the proposed self-oscillation identification method.

$$K_I = \frac{\tilde{I}_r}{a_3} \quad (8)$$

$$K_P = \frac{a_1}{a_3} \tilde{I}_r \quad (9)$$

$$K_D = \frac{a_2}{a_3} \tilde{I}_r - \varepsilon = \frac{a_2}{a_3} \tilde{I}_r - \tilde{k}_{rr} |\dot{\Psi}| \quad (10)$$

Stability issues for the proposed controller have been described in detail in Miskovic et al. (2008). Here we will assume that the stability can be compromised due to false identification of the system's parameters, giving the closed loop equation in the form (11) where I_r and \tilde{I}_r are real and identified moments of inertia respectively, and $\varepsilon = k_{rr} |\dot{\Psi}|$ and $\tilde{\varepsilon} = \tilde{k}_{rr} |\dot{\Psi}|$ with k_{rr} and \tilde{k}_{rr} being real and identified drag coefficients, respectively.

$$\frac{\Psi}{\Psi_{ref}} = \frac{1}{\frac{\tilde{I}_r}{I_r} a_3 s^3 + [a_2 + a_3 \frac{\varepsilon - \tilde{\varepsilon}}{\alpha}] s^2 + a_1 s + 1} \quad (11)$$

The closed loop will be stable if condition (12) is fulfilled.

$$|\dot{\Psi}| < \frac{\frac{a_2}{a_3} \tilde{I}_r - \frac{1}{a_1} I_r}{\tilde{k}_{rr} - k_{rr}}. \quad (12)$$

This condition is implemented within the controller as a limiter to the derivation channel. Under the assumption that \tilde{k}_{rr} is within 20% of k_{rr} and that \tilde{I}_r is within 10% of I_r , the constraint can be set to $|\dot{\Psi}| < \frac{2}{3} \frac{\tilde{I}_r}{k_{rr}} \frac{9a_1 a_2 - 10a_3}{a_1 a_3}$.

3. Implementation issues

The complete scheme of implementation can be presented with Fig. 2. The basic parts of the controller scheme are the controller and the self-oscillation execution and monitoring system. The main goal of the self-oscillation execution and monitoring system is to automatically gather self-oscillation data, calculate controller parameters and switch between control and self-oscillation mode.

3.1. Controller Implementation

Once the controller is written in a discrete form given with (13)

$$\tau_{N,k} = \tau_{N,k-1} + K_I T_s e_k - K_P \Delta \Psi_k - K_{D,k}^* \Delta r_k \quad (13)$$

where $e_k = \Psi_{ref}(k) - \Psi(k)$, $\Delta \Psi_k = \Psi(k) - \Psi(k-1)$, $\Delta r_k = r(k) - r(k-1)$ and the time variable parameter $K_{D,k}^* = K_D - k_{rr} |r(k)|$, the issue of calculating the yaw rate, i.e. heading derivative remains. In this paper we will demonstrate the results using the controller with yaw rates obtained in two ways: using the Euler backward difference and using the Kalman filter.

Using the Euler backward difference (EB Controller)

The classical procedure is to perform the backward Euler discretization method on the derivative $s\Psi(t)$ yielding $r(k) = \frac{\Psi(k) - \Psi(k-1)}{T_s}$. Even though this is the simplest method, many problems concerning noise amplification are involved. Therefore this procedure should be avoided.

Using the Kalman filter (KF Controller)

If system equation (1) is linearized and written in a discrete state-space form, than a Kalman filter can be obtained where $\underline{x}_i = [\Psi_i \quad r_i]^T$ is the state vector.

When the new measurement from the gyro is available (every 0.5s) the Kalman filter measurement matrix is $\underline{h} = [1 \quad 0]^T$ and in other cases $\underline{h} = [0 \quad 0]^T$. It

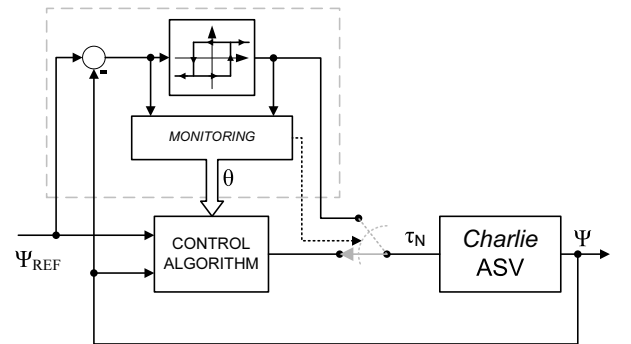


Fig. 2. Implementation scheme of controllers tuned according to self-oscillation experiments.

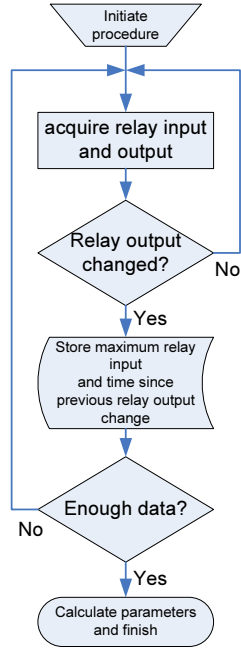


Fig. 3. Flow diagram of the self-oscillation monitoring system.

should be mentioned that the compass data has an update frequency of 2Hz while Kalman filter estimates values at the frequency 8Hz. This means that EB controller will have the refresh rate of 0.5s while KF controller will refresh its output every 0.125s.

3.2. Monitoring and Identification System

The Monitoring and Identification System takes relay output and relay input as input parameters, and outputs identified system parameters and switching signal. As it can be seen from Fig. 3 after the relay has been inserted in the closed loop, the data collection is initiated. Based on the relay output data, every time a relay output changes, the maximum value in the previous half-period and the duration of the previous half-period is recorded. This data is gathered until a predefined number of measurements (in this paper it is five) has a standard deviation less than a predefined value (in this paper it is 10%). This means that the obtained data is reliable and can be used for identification procedure. This leads the algorithm to the phase in which the system parameters are calculated and the controller with the new parameters is inserted in the closed loop.

4. Experimental results

Experimental tests have been carried out at Genova-Prá harbor with the Charlie USV. Numerous self-oscillation

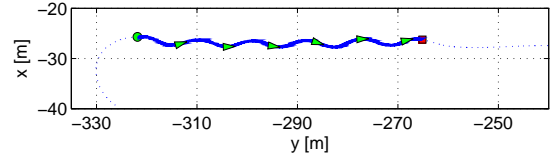


Fig. 4. Charlie's path during one of the self-oscillation experiments (green circle marks the beginning and red square the end of data recording, dotted line is the path before and after the experiment).

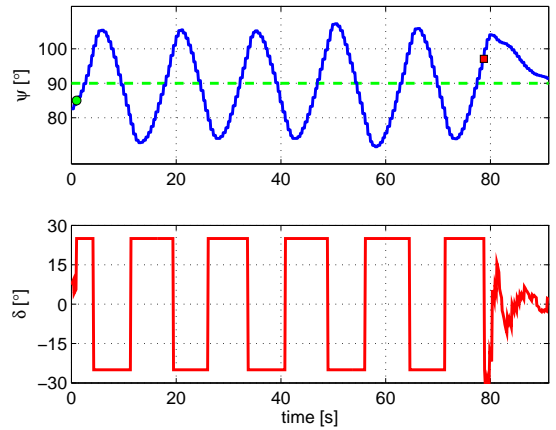


Fig. 5. Charlie's heading and rudder angle during one of the self-oscillation experiments (green circle marks the beginning and red square the end of data recording).

experiments were run and the data obtained was used to determine the model of the vehicle and to tune controller parameters. Some self-oscillation experiment data are shown in Table 1. The columns in the table are as follows: relay output ($\delta \cdot n^2$), relay hysteresis width (x_a), modified relay hysteresis width (x_a^*), self-oscillation magnitude (X_m), period of self-oscillations (T), value of the bias during the experiment according to (4) (τ^*) in relation to the relay output, identified moment of inertia (\tilde{I}_r), identified constant drag (\tilde{k}_r) and identified linear drag (\tilde{k}_{rr}).

During the experiment the vehicle was excited with a constant force equivalent to $n^2 = 36V$ and the relay output was either 20° or 25° . In the cases when smaller relay outputs were used, the data were difficult to obtain, i.e. the automated self-oscillation monitoring system would never stop due to inconsistent data (it would take long time to fulfill the self-oscillation acquiring process). The reason for this is the external disturbance and system noise. In Miskovic et al. (2007c) it is shown that the ratio between the magnitude of obtained self-

Tab. 1. Self-oscillation experiment results from Charlie USV

$\delta \cdot n^2$	$x_a [^\circ]$	$x_a^* [^\circ]$	$X_m [^\circ]$	$T [s]$	$\frac{\tau}{n^2 \delta} \cdot 100\%$	\tilde{I}_r	\tilde{k}_r	\tilde{k}_{rr}
$20^\circ \cdot 36V$	5	5.70	10.18	11.83	19.24	264.24	95.032	1186.329
	10	10.94	14.65	15.83	20.38	264	117.69	1365.77
$25^\circ \cdot 36V$	5	6.58	11.56	11.55	13.85	275.44	103.59	1111.54
	10	11.32	16.3	14.93	6.87	285.51	115.93	1140.4

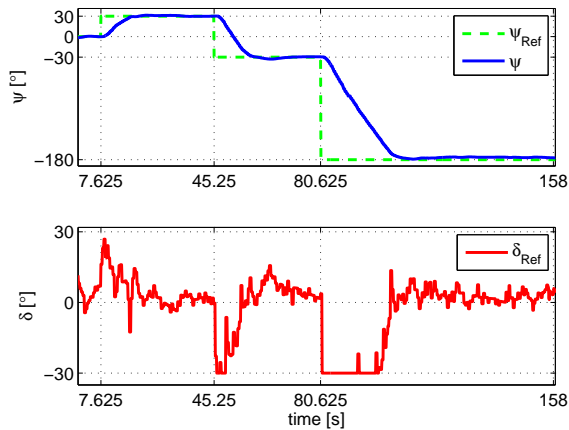


Fig. 6. Heading and rudder angle with the EB controller.

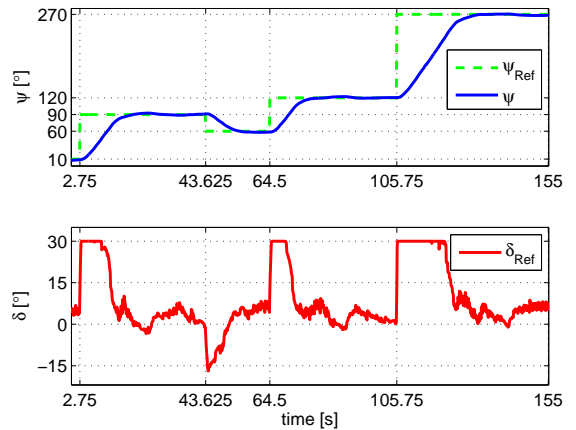


Fig. 7. Heading and rudder angle with the KF controller.

oscillations (X_m) and the hysteresis width (x_a) should be around 1.5. The results show that this was more or less accomplished. The identified bias term can be a good indicator of the disturbance that was present in the system during the experiment. In this case, the disturbance can appear due to sea currents or vehicle asymmetries. However, it can be shown that the biased value does not influence the quality of the identified data significantly.

From experiments in Table 1 it can be seen that the vehicle's moment of inertia is consistent. The constant drag has been identified using (14). A detailed derivation of this formula can be found in Miskovic et al. (2007b) and Miskovic et al. (2007c).

$$k_r = -\frac{Q_N(X_m)}{\omega} \quad (14)$$

This parameter is calculated in order to check if a linear model fits the obtained data better than the nonlinear model. It can be seen from Table 1 that the data more consistently fit (3) rather than (14). Therefore, the assumption from the beginning that the process can be described using (6) is valid.

The last experiment from Table 1 was used to tune the controllers and it is shown in Fig 5 where heading (ψ) and commanded rudder angle (δ) are shown. Fig. 4 shows the path of the vehicle during the same experi-

ment. The controller was automatically tuned so that the desired closed loop function is Bessel filter with characteristic frequency $0.45s^{-1}$. The step response of the desired model has a time of first maximum at around 15s and an overshoot of about 1%. The model was chosen in such a way that the rudder signal is not noisy in steady state (slower model) but that transient response is fast enough (faster model).

Results with EB and KF controllers are shown in Fig. 6 and Fig. 7, respectively. In both cases the behavior of the system is satisfactory. The main difference between the two cases is in rudder angle noise level. In the following part noise attenuation will be observed by finding the spectra of the rudder angle for the two cases.

The rudder angle signals from Fig. 6 and Fig. 7 were first filtered out with a high pass 8th order Butterworth filter with a cutoff frequency $\frac{3}{4}\pi \frac{rad}{sample}$. This way only the high frequency components remain in the signal. Now the power spectrum density was estimated using the Welch's method. The results for both controllers are shown in Fig. 8. Now it is clear that in the case of KF controller, the noise is smaller, hence the controller action is less jerky.

Therefore, if simpler controller is needed (because of memory limitations) EB controller is sufficient. How-

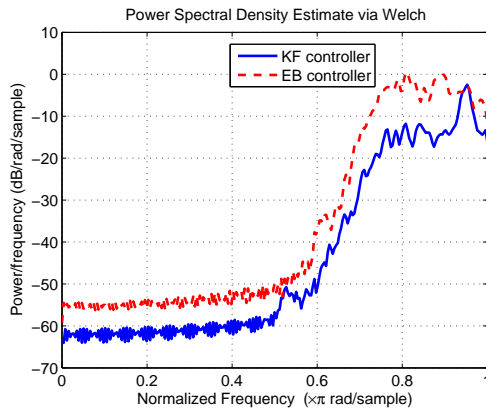


Fig. 8. Power spectrum density of rudder angle signals for the case of EB and KF controllers.

ever, if there is the possibility of implementing a Kalman filter as an addition to the controller, it is advised.

5. Conclusion

This paper has demonstrated how self-oscillation identification method can be used on tuning heading controllers for marine surface vehicles. The greatest advantage of the proposed method is the fact that it is not time-consuming and that it can be simply implemented. It has also been shown that good results are obtained even when external disturbances are present, making the experiment itself feasible in real conditions. The implementation of two controllers is described: a classical controller which calculated the derivative by using Euler backward method (EB controller), and a controller with a Kalman filter (KF controller). The greatest advantage of the EB controller is its simplicity, while the disadvantages are higher noise level in actuators. The KF controller is somewhat more complex, but the noise level is reduced. Having this in mind, the KF controller is advised where possible.

6. Acknowledgments

The work was carried out in the framework of the research project "RoboMarSec - Underwater robotics in sub-sea protection and maritime security" supported by the Ministry of Science, Education and Sport of the Republic of Croatia (Project No.036-0362975-2999). The research was partially funded from the scholarship awarded by the Italian Government and the Ministry of Science, Education and Sport of the Republic of Croatia. The authors would like to thank Giorgio Bruzzone and Edoardo Spirandelli for their fundamental support in the

development and operation of the Charlie USV, and *Associazione Prà Viva* for their kind help in allowing the experiments to take place on their ground.

7. References

- Caccia, M., G. Indiveri and G. Veruggio. 2000. Modelling and identification of open-frame variable configuration underwater vehicles, *IEEE Journal of Ocean Engineering*, 25(2), pp 227-240.
- Caccia, M., G. Bruzzone and R. Bono. 2006. Modelling and identification of the Charlie2005 ASC, *Proc. of IEEE 14th Mediterranean Conference on Control and Automation*.
- Caccia, M., R. Bono, G. Bruzzone, G. Bruzzone, E. Spirandelli, G. Veruggio, A. Stortini and G. Capodaglio. 2005. Sampling sea surface with SESAMO, *IEEE Robotics and Automation Magazine*, 12(3), pp 95-105.
- Fossen T.I. 1994. *Guidance and Control of Ocean Vehicles*, John Wiley & Sons.
- López, E., F.J. Velasco, E. Moyano and T.M. Rueda. 2004. Full-scale manoeuvring trials simulation, *Journal of Maritime Research*, 1(3), pp 37-50
- Miskovic, N., Z. Vukic and M. Barisic. 2007. Identification of coupled mathematical models for underwater vehicles, *Proc. of the OCEANS'07 Conference*.
- Miskovic, N., Z. Vukic and M. Barisic. 2007. Transfer function identification by using self-oscillations, *Proc. of the 15th Mediterranean Conference on Control and Applications*.
- Miskovic, N., Z. Vukic, M. Barisic and P.P. Soucaos. 2007. AUV identification by use of self-oscillations, *Proc. of the CAMS'07 Conference*.
- Miskovic, N., Z. Vukic and E. Omerdic. 2008. Control of UUVs Based upon Mathematical Models Obtained from Self-Oscillations Experiments, *Proc. of the NGCUV'08 Conference*.
- Ridao, P., A. Tiano, A. El-Fakdi, M. Carreras and A. Zirilli. 2004. On the identification of non-linear models of unmanned underwater vehicles, *Control Engineering Practice*, 12, pp 1483-1499.
- Stipanov, M., N. Miskovic, Z. Vukic and M. Barisic. 2007. ROV autonomization - yaw identification and Automarine module architecture, *Proc. of the CAMS'07 Conference*.
- Vukic, Z., Lj. Kuljaca, D. Donlagic and S. Tesnjak. 2003. *Nonlinear Control Systems*, Marcel Dekker, New York.
- Vukic, Z., and Lj. Kuljaca. 2005. *Automatic Control - Analysis of Linear Systems (in Croatian)*, Kigen, Zagreb.